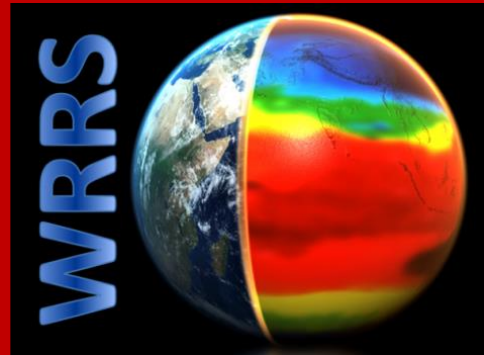


A Global Hot Spot Analysis (Getis-Ord Gi*) of Groundwater Storage Change using GRACE Satellite and GIS-Based Spatial Statistical Analysis



Khalil A. Lezzaik and Adam M. Milewski
Department of Geology, University of Georgia, Athens, GA, USA

Abstract:

Global groundwater is declining as a function of over extraction, pollution, and climate change effects on precipitation. While the dwindling of groundwater resources has been noticed, a holistic and accurate assessment of groundwater storage change (GWSC) patterns and distributions has never been conducted given the global scale of the assessment and the paucity of in-situ monitoring systems worldwide. Therefore, in this study, alternative remote sensing approaches are utilized to not only delineate the distribution of global GWSC but to also observe the relationships between climatic factors and GWSC.

NASA's gravity recovery and climate change experiment (GRACE) mission satellite was used to derive GWSC estimates for the purposes of identifying spatial clusters of hot spot (HS) and cold spot (CS) GWSC values. A $10^\circ \times 10^\circ$ grid was utilized to generate GWSC estimates by isolating GLDAS - derived surface water parameters from GRACE-derived total water storage change signal. Resultant GWSC estimates underwent a hot spot (Getis-Ord Gi*) analysis to map statistically significant spatial clusters of GWSC HS/CS with a 99% confidence interval. Moreover monthly TRMM 3B43 datasets were similarly analyzed to produce HS/CS precipitation areas that were compared to GWSC hot spot analysis results.

In Africa, CS were located in Madagascar and the Nile river basin ($Z < -4.1$). Alternatively a HS area was established in Angola and Zambia ($Z > 5.6$). In Asia, CS were primarily centered in Iraq and western Iran, and in Northern India and Nepal ($Z < -7.5$); whereas HS domains were dispersed in western Turkey, southern India, central Asia region and southeast China ($Z > 6$). In Europe, CS regions were located in the British Isles, western French coast, eastern Ukraine, and southwestern Russia ($Z < -3.28$). Contrastingly, HS areas were located primarily in southeast Europe, and in Portugal and southern Spain ($Z > 4$). In Australia, the CS area is in northwestern Australia ($Z < -8.3$); whereas a HS area was established on the central eastern coast ($Z > 7$).

Precipitation and GWSC HS analysis results displayed direct correspondence in several cases (e.g. Nile river basin and eastern Ukraine), while a few areas displayed a disassociation (e.g. Portugal and southern Spain, northwestern Australia), thus indicating an influence of anthropogenic factors on GWSC.

Objectives:

The primary objective of this study is to use GRACE ensemble datasets (arithmetic mean of JPL, CSR, and GFZ datasets), precipitation datasets (TRMM 3b43 V7), and land surface parameters (GLDAS-2.0 NOAH) to:

1. Generate and delineate the distribution of groundwater storage change using hot spot analysis
2. Determine the relationship between precipitation estimates and groundwater storage change using spatial regression analysis
3. Quantify groundwater storage change (GWSC) of major aquifers globally.

Methodology

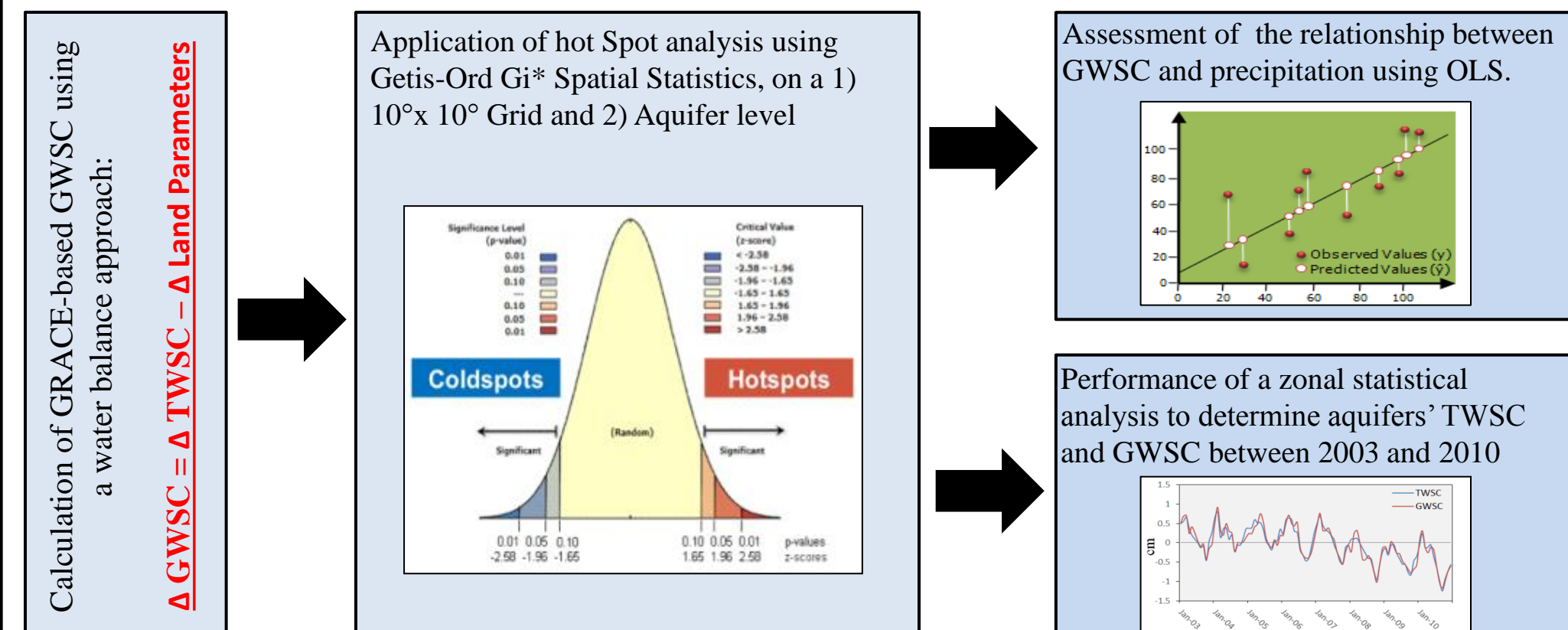


Fig. 1. Diagram displaying the different methodological procedures in sequential order.

Results:

1a. Global Hot Spot Analysis of GRACE- Based GWSC at $10^\circ \times 10^\circ$ Grid Level

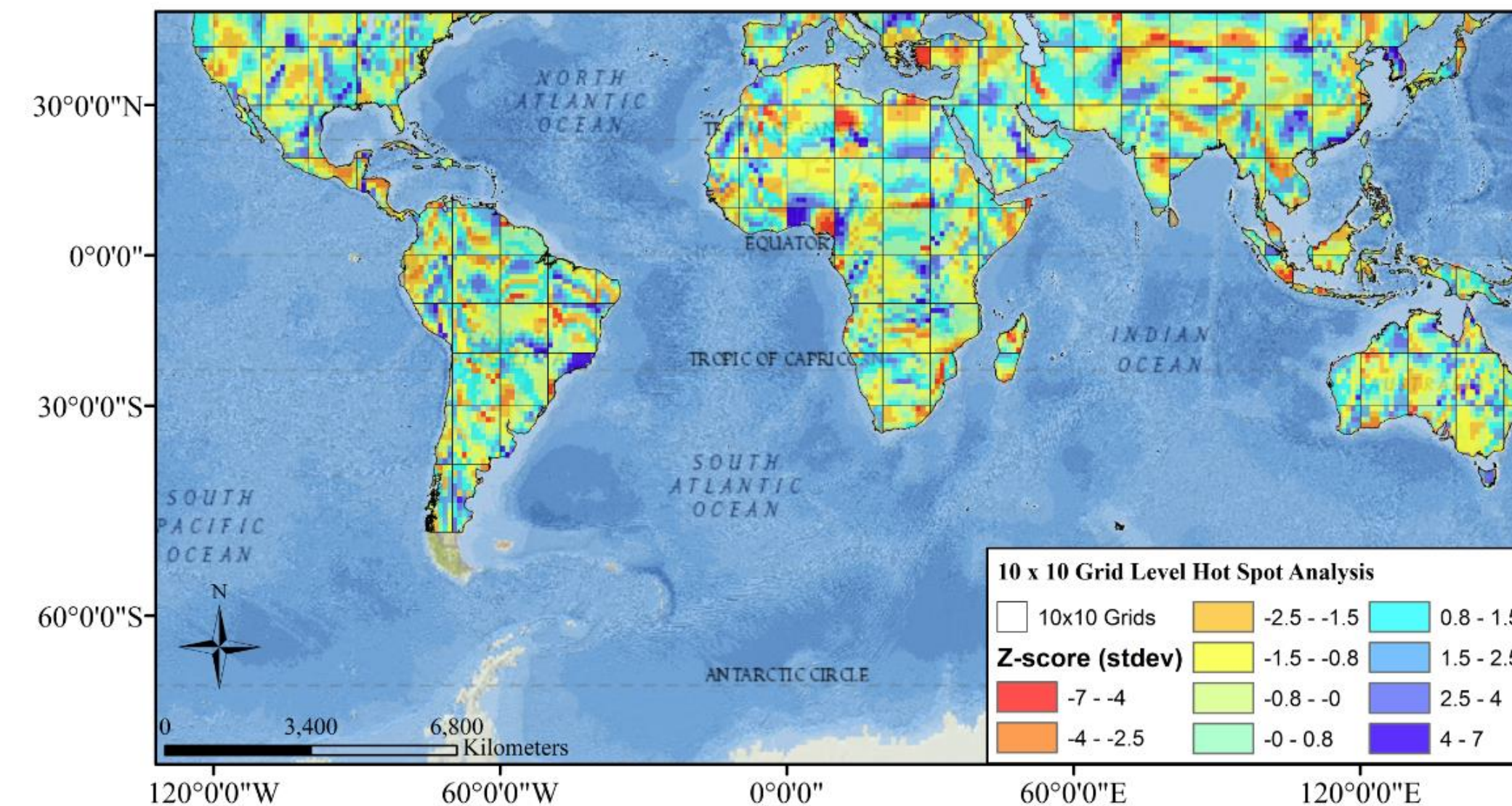


Fig. 2. Global GWSC map displaying the spatial results of the hot spot analysis on a grid level. The bright red color represent “cold spot” areas with a spatial concentration of low GWSC values. Alternatively dark blue colors represent “hot spot” areas with a spatial clustering of high GWSC values.

1b. Global Hot Spot Analysis of GRACE- Based GWSC at Aquifer Level

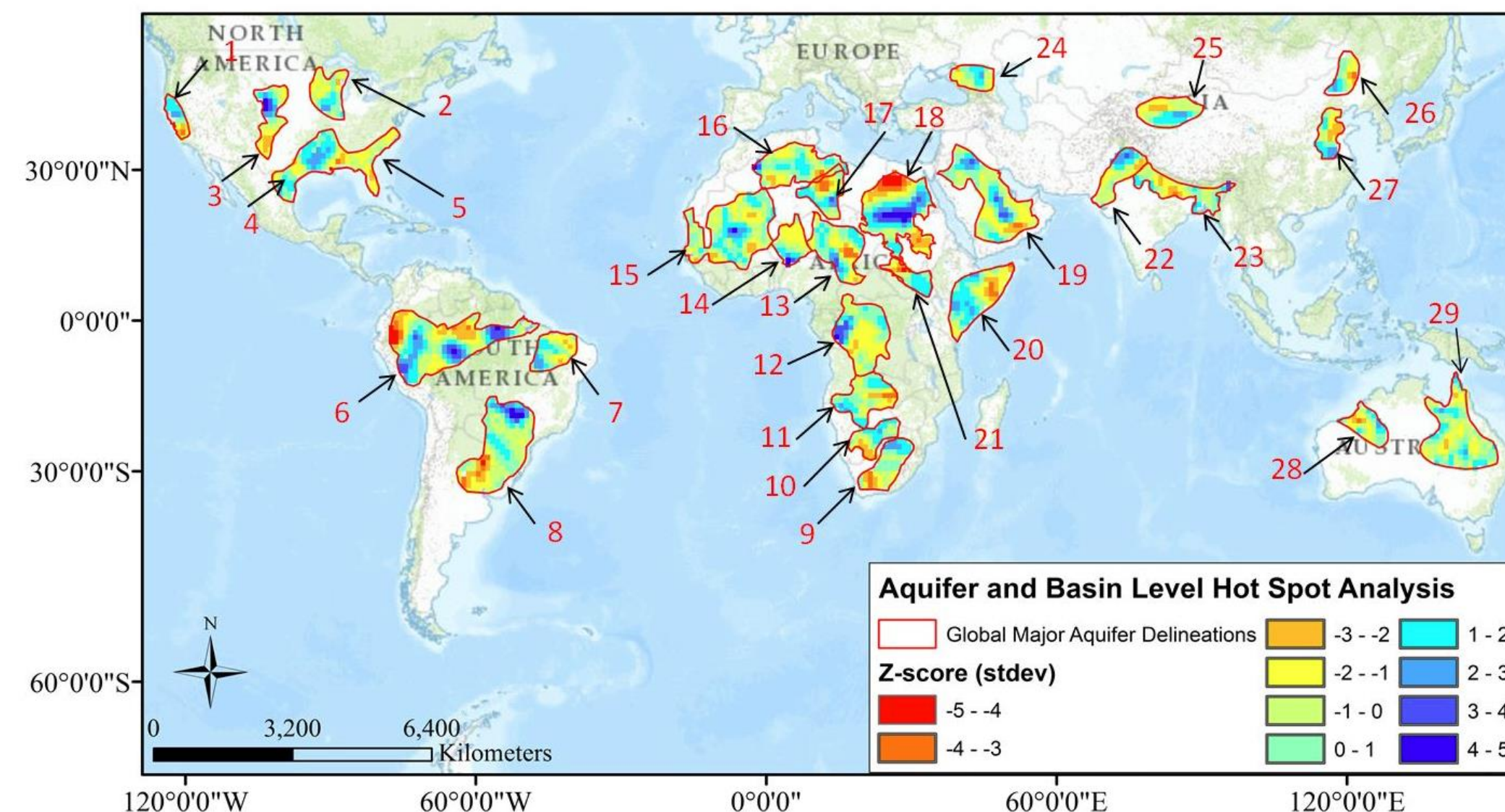


Fig. 3. Global GWSC map displaying the spatial results of the hot spot analysis on an aquifer level. The red numbering refers to the following aquifer systems: 1) Central California Valley 2) Cambrio-Ordovician 3) Ogallala High Plains 4) Gulf Coastal 5) Atlantic Coastal 6) Amazonas 7) Maranhao 8) Guarani-Mercosul 9) Karoo 10) Lower Kalahari 11) Upper Calahari 12) Congo 13) Lac Chad 14) Iullemeden – Irhazer 15) Iullemeden-Irhazer 16) Northwestern Sahara 17) Murzuk-Djado 18) Nubian 19) Arabian 20) Ogaden-Juba 21)Umm Ruwaba 22) Indus 23) Indus-Ganges-Brahmaputra 24) Northern Caucasus 25) Tarim 26) Song-Liao Plain 27) Northern China 28) Canning Basin 29) Artesian Grand Basin.

2. Statistical Correlation Between Precipitation and GWSC

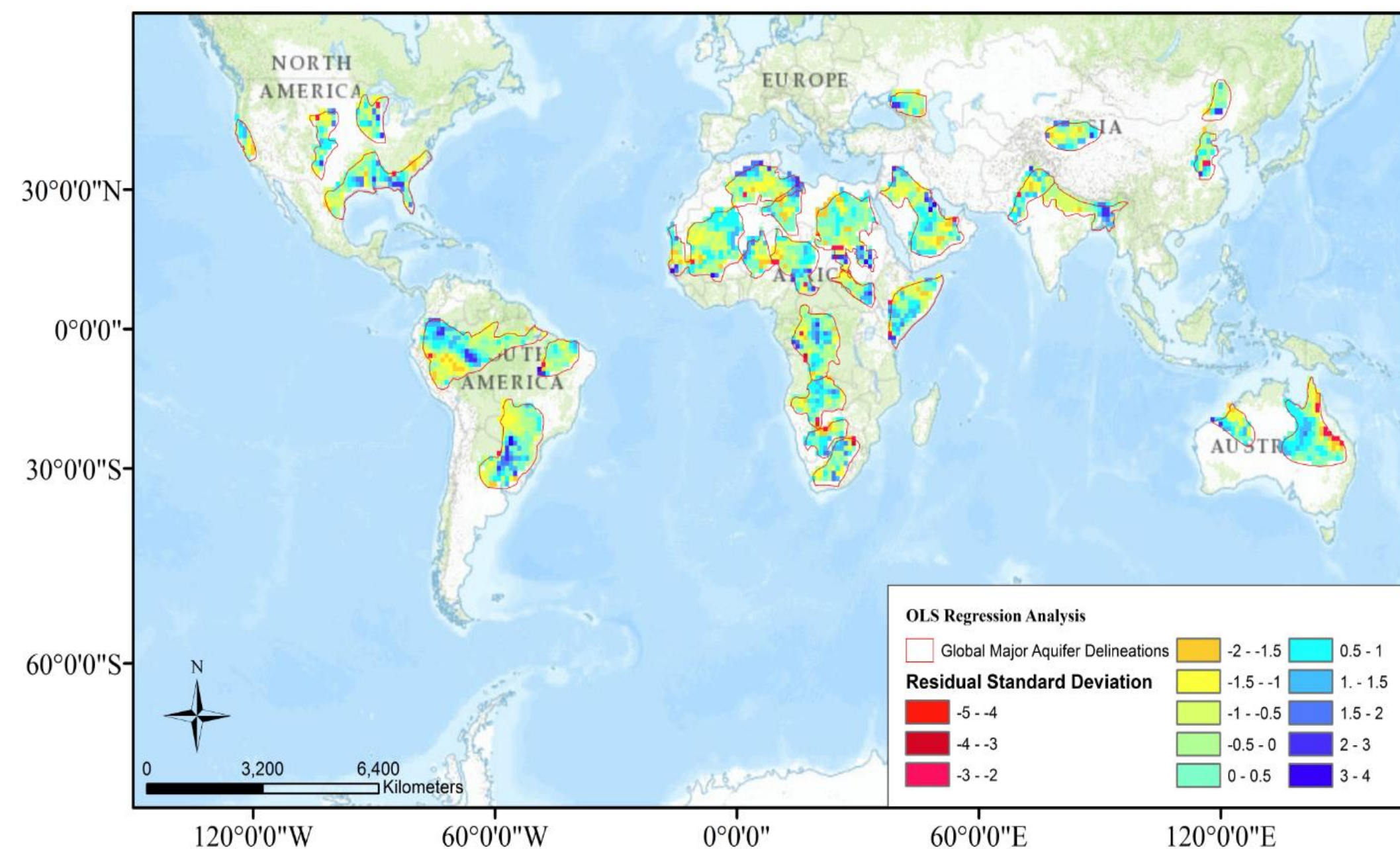


Fig. 4. Global map displaying the relationship between precipitation (explanatory variable) and GWSC (dependent variable) based on residual standard derivation estimates generated by an ordinary least squares regression model. Light yellow, blue, and green colors correspond to areas with high precipitation-GWSC correlation. Dark red and blue colors correspond to areas with low precipitation-GWSC correlation.

3. Quantification of Cumulative GWSC in Major Large Aquifer Globally between 2003 and 2010

Aquifer/ Basin	Area (sq. km)	GWSC (water column, cm)	GWSC (volumetric, km3)
Northern Caucasus Basin	288825	-66.53	-192.17
Central California Valley Aquifer System	419040	-35.10	-147.10
Umm -Ruwwaba Aquifer	470534	18.72	88.10
Song - Liao Plain	477958	8.80	42.08
Low Kalahari - Stampriet Basin	494316	6.40	31.64
Iullemeden -Irhazer Aquifer System	553636	25.19	139.47
Cambro-Ordovician Aquifer System	614542	40.91	251.39
Murzuq Djado Basin	617341	-6.02	-37.13
Karoo Basin	674316	11.54	77.78
Tarim Basin	711981	14.38	102.35
Indus Basin	752482	-20.03	-150.73
Ogallala High Plains Aquifer	766478	-32.77	-251.18
Maranhao Basin	777693	-77.69	-604.22
High Kalahari Cuvelai	987577	86.15	850.83
North Western Sahara Aquifer System	1096982	-4.41	-48.41
Indus - Ganges - Brahmaputra Basin	1142907	-3.77	-43.06
Lac Chad Basin	1153914	13.34	153.91
Canning Basin	1249850	-2.67	-33.33
Ogaden - Juba Basin	1468133	24.96	366.39
Congo Basin	1589759	122.91	1954.00
Taoudeni -Tanezzrouft Basin	1851101	33.22	614.85
Nubian Aquifer System	1979482	25.13	497.54
Arab Aquifer Basin	1987873	-5.31	-105.62
Atlantic Ocean and Gulf Coastal Plains Aquifer	2112984	108.67	2296.08
Guarani - Mercosul Aquifer System	2240517	110.65	2479.22
Amazona Basin	3534833	-91.71	-3241.65
Artesian Grand Basin	5918896	82.71	4895.25
Total Groundwater Storage Change	35933950	388	9986

Aquifer / Basin	Adjusted R^2
Amazonas Basin	0.99
Arab Aquifer System	0.92
Artesian Grand Basin	0.93
Atlantic Ocean and Coastal Plains Aquifer	0.96
Cambrio-Ordovician Aquifer System	0.96
Canning Basin	0.98
Central California Valley Aquifer System	0.61
Congo Basin	0.94
Guarani (or Mercosul) Aquifer System	0.99
High Kalahari Cuvelai Basin	0.98
Indus Basin	0.98
Indus-Gange-Brahmaputra Basin	0.22
Iullemeden – Irhazer Aquifer System	0.97
Karoo Basin	0.97
Lac Chad Basin	0.88
Low Kalahari – Stampriet Basin	0.27
Maranhão Basin	0.95
Murzuk – Djado Basin	0.58
Northern Caucasus Basin	0.96
Northern China Aquifer System	0.98
North-Western Sahara Aquifer System	0.84
Nubian Aquifer System	0.99
Ogaden-Juba Basin	0.98
Ogallala Aquifer (High Plains)	0.99
Song-Liao Plain	0.98
Taoudeni – Tanezzrouft Basin	0.98
Tarim Basin	0.69
Umm Ruwaba Aquifer	0.5

Tab. 1. Adjusted R-squared values reflecting the correlation between precipitation and GWSC in different aquifer systems globally.

Future Work

- Examining the relationship between GWSC and environmental variables such as vegetative cover, soil, and topography using spatial exploratory regression.

Acknowledgments

- The Geological Society of America
- University of Georgia Office of the Vice President for Research
- Watts-Wheeler Scholarship Fund